Light-Driven Ecological-Evolutionary Dynamics in a Synthetic Replicator System

Kai Liu[1], Alex W. P. Blokhuis[1], Chris van Ewijk[2], Armin Kiani[1], Juntian Wu[1], Wouter H. Roos[2], Sijbren Otto[1]*

[1]Centre for Systems Chemistry, Stratingh Institute, University of Groningen, Groningen 9747 AG, The Netherlands

[2]Molecular Biophysics, Zernike Institute for Advanced Materials, University of Groningen, Groningen 9747 AG, The Netherlands

*Corresponding author. Email: s.otto@rug.nl

Abstract

Natural selection is the cornerstone of Darwinian evolution and acts on reproducing entities exhibiting variations that can be inherited and selected for based on, among others, interactions with the environment. Conversely, the replicating entities can also affect their environment generating a two-way feedback on evolutionary dynamics. The onset of such ecological-evolutionary dynamics marks a stepping stone in the transition from chemistry to biology. Yet the bottom-up creation of a molecular system that exhibits ecological-evolutionary dynamics has remained elusive. Here, we describe the onset of such dynamics in a minimal system containing two synthetic self-replicators. The replicators are capable of binding and activating a cofactor, enabling them to change the oxidation state of their environment through photoredox catalysis. The replicator distribution adapts to this change and, depending on light intensity, one or the other replicator prevails. In both cases the replicator distribution evolves towards higher dynamic kinetic stability, rooted in a faster replication rate under the specific environmental conditions. This study opens the world of chemistry to evolutionary dynamics that has until now been restricted to biology.

Introduction

Darwinian evolution is an unrivalled creative engine. The complexity and ingenuity of the diverse forms of life that surround us today underscores how powerful evolution is at inventing. Mankind has started harnessing the power of evolution centuries ago (through breeding of crops and livestock), and continues to do so to date. With the exception of the use of evolutionary methods in *in-silico* systems (i.e. evolutionary algorithms[1]), the utilization of Darwinian concepts has remained relatively close to biology and has relied strongly on biomolecules. Take, for example, the directed evolution of proteins, utilizing the corresponding genes to drive structure variation and relying on biology's transcription/translation machinery for protein synthesis.[2,3] Achieving Darwinian evolution of self-replicating molecular systems without having to make use of biomolecules has so far not been realized. Yet, extending Darwinian principles to systems of completely synthetic molecules would open up a world of opportunities for developing new functional chemical systems.[4]

Implementing Darwinian evolution in synthetic chemical systems ideally requires: (i) that these systems reproduce; (ii) that reproduction is accompanied by variation (non-perfect "mutant" copies are made); and (iii) that different variants have a different chance of surviving in an out-of-equilibrium regime in which reproduction and destruction take place (similar to natural selection).

In biology, natural selection of phenotypic features of organisms is often based on the interaction of these features with the environment, causing organisms to adapt to their environment. Such dynamics has been observed in the laboratory with bacteria, viruses, or RNA molecules.[5-7] In turn, such evolutionary change in phenotype can cause a change in the environment, leading to ecological-evolutionary dynamics that can occur between organisms and their (a)biotic environments.[8,9]

In chemistry, several synthetic self-replicating systems have been developed.[10-12] The capacity of these systems for undergoing Darwinian evolution has received only little attention.[13] It is well established that environmental influences (e.g. pH,[14] ionic strength,[15] solvent,[16] and light[17,18]) can affect replication dynamics and even the molecular composition of the replicator. However, this behavior was mostly observed in closed systems that are approaching the thermodynamically most stable state, where the chemical equivalent of natural selection does not readily occur due to the absence of a process that destroys or removes a subset of replicators. It is essential to impose an out-of-equilibrium state[19-24] onto self-replicating systems that allows for selection based on dynamic kinetic stability[25,26] as opposed to thermodynamic stability. A continuous input of energy and/or material is needed to maintain an out-of-equilibrium replication-destruction regime. Such regime can be implemented chemically,[27] but also physically, using a continuously stirred tank reactor,[28,29] but has not yet yielded ecological-evolutionary dynamics.

We reasoned that achieving such dynamics should be possible by making use of replicators that are able to catalyze chemical reactions (in addition to their own replication), that change the nature of the molecules in their environment,[30-33] which, in turn may impact on the replication process. We recently developed a replicator system capable of recruiting a cofactor and enhancing its activity as a photoredox catalyst.[32] The replicator ($\mathbf{1}_6$; Figure 1) emerges from a small dynamic combinatorial disulfide library[34] formed upon oxidation of building block **1** and is driven by assembly of the replicator into stacks, held together by β-sheet formation between the peptides.[35] Mechanical agitation allows for exponential replication.[36] Fibers of $\mathbf{1}_6$ can bind to different cofactors and enhance their activity in photoredox catalysis. This potential ability to change the oxidation state of the reaction medium prompted us to explore how such change affects the relative replication efficiency of competing replicators.

We now report a minimal system of two competing replicator mutants, where selection based on dynamic kinetic stability takes place in response to changes in the environment: Different

light intensities yield different replicator distributions. The replicators utilize light to modify the oxidation state of their environment. In turn, this oxidation state determines which of the two replicators wins the competition for a common building block in a replication-destruction regime. This environment-dependent selection for the replicator with the highest dynamic kinetic stability represents the first example of a rudimentary ecological-evolutionary dynamics in a synthetic replicator system and shows how such dynamics can manifest even in relatively simple abiotic systems.

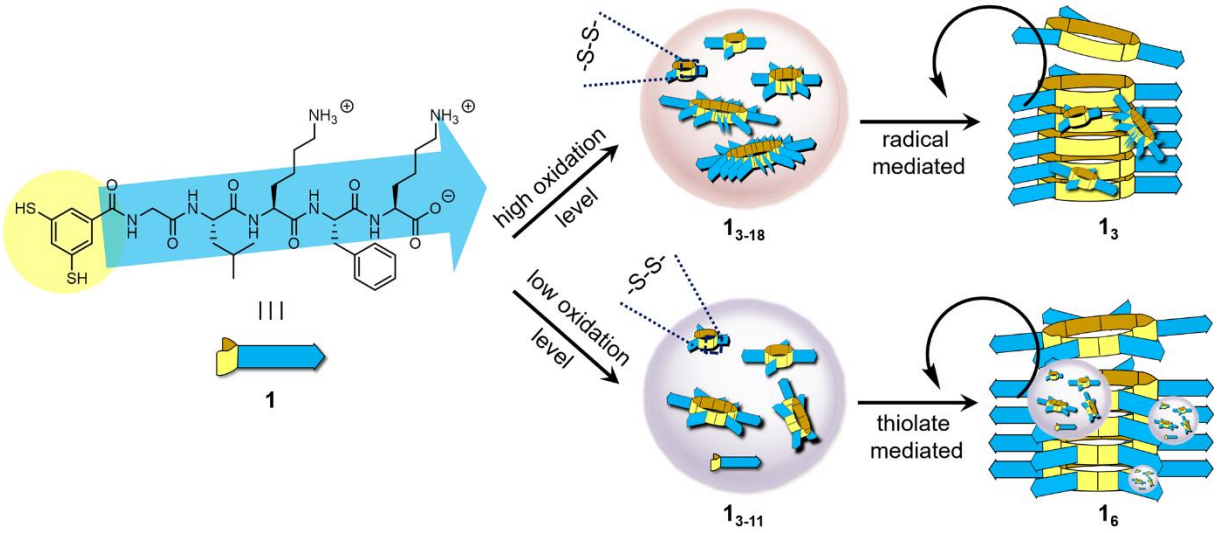

Figure 1. Competition by replicators $\mathbf{1}_3$ and $\mathbf{1}_6$ for a common building block. At high oxidation level replicator $\mathbf{1}_3$ prevails, while at low oxidation level $\mathbf{1}_6$ dominates, which is partially a result of different oxidation levels leading to different precursor aggregates from which the competing replicator grow with different efficiencies and partially due to different replicators utilizing different mechanisms for disulfide exchange that respond differently to oxidation level.

Results and discussion

We hypothesized that ecological-evolutionary dynamics could emerge in a system where different replicators compete for a common resource and where their replication is affected differently by changes in the environment that are mediated by these replicators. Having shown previously that self-replicators can alter the redox state of molecules in their

environment,[32] we set out to identify replicators that would show different replication efficiencies at different redox states. The serendipitous observation that treating dithiol building block **1** with one equivalent of perborate gave rise to fibers composed of macrocyclic disulfide $\mathbf{1}_3$, while slower oxidation by oxygen from the air produced fibers of $\mathbf{1}_6$, encouraged us to investigate how both systems respond to the oxidation level of the medium. However, we first characterized the $\mathbf{1}_3$ system in more detail and verified whether it is indeed a self-replicator under these conditions. Note that we already established this previously for $\mathbf{1}_6$ under the conditions used.[32]

Characterization of replicator $\mathbf{1}_3$

Treating a solution of dithiol **1** (1.0 mM) in borate buffer (50 mM, pH 8.2) with excess sodium perborate (2.0 mM) rapidly and completely oxidized it into a series of macrocycles with ring sizes ranging from 3 to 18, as evident from ultra-performance liquid chromatography-tandem mass spectrometry (UPLC-MS/MS) analysis (Figure S1b and S2-S13). Stirring this sample converted this mixture into $\mathbf{1}_3$ (Figure 2A). Apparently disulfide exchange is taking place in absence of thiolates. Such behavior is precedented[37] and has been reported to occur through a radical-mediated mechanism.[38] Indeed, addition of a radical trap diminished the rate of replication of $\mathbf{1}_3$ (Figure S37a). Note that, in our experience, the rate of replication of larger-ring replicators, including $\mathbf{1}_6$ is prohibitively slow in fully oxidized samples. The conversion into $\mathbf{1}_3$ is accompanied by an increase in turbidity, indicative of the formation of aggregates. Transmission electron microscopy (TEM) confirmed the presence of laterally associated fibers in the resulting $\mathbf{1}_3$ solution (Figure 2D). We further characterized these fibers using circular dichroism (CD) spectroscopy and thioflavin T (ThT) fluorescence assays. The CD spectrum of the $\mathbf{1}_3$ solution shows negative helicity around 213 nm (Figure S17), indicative of β-sheet structure.[39] ThT assays showed an increase in emission intensity (Figure S18), which is indicative of an amyloid-fibril-like structure.[40] The self-assembly of $\mathbf{1}_3$ appears essential for the conversion of nearly all the library members into $\mathbf{1}_3$ fiber, as evident from the

fact that a mixture formed upon oxidation of building block of reduced hydrophobicity (thereby less prone to self-assembly) did not lead to the dominance of a specific macrocycle size (Figure S1c).

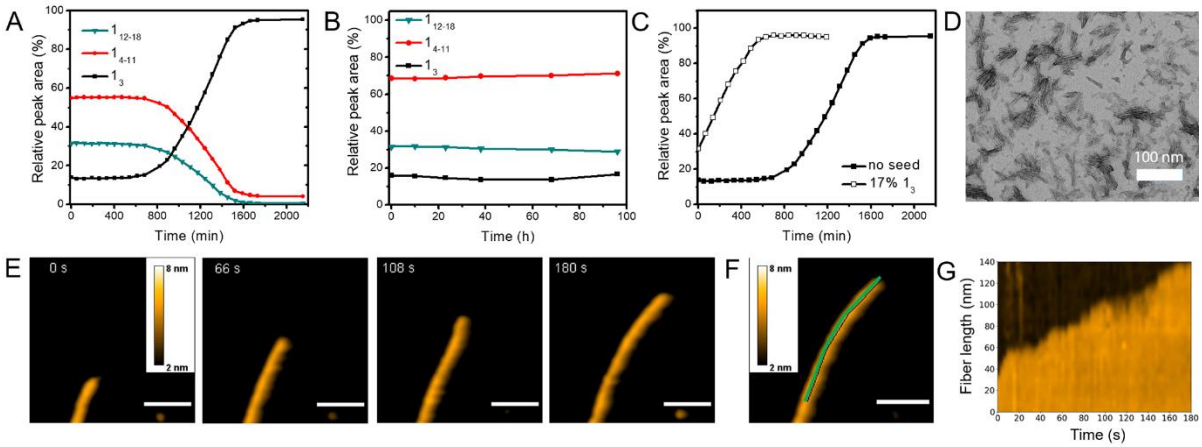

Figure 2. Characterization of replicator $\mathbf{1}_3$. Change in product distrubution with time of a solution made by a mixing of **1** (1.0 mM) and sodium perborate (1.2 mM) in borate buffer (50 mM, pH 8.2) (**A**) while stirred at 1200 r.p.m and (**B**) prepared without agitating at 25°C. (**C**) Growth of $\mathbf{1}_3$ in a fully oxidized "food" solution (1.0 mM in **1**) in borate buffer (50 mM, pH 8.2) in the absence of seed (filled circles) or seeded with $\mathbf{1}_3$ fiber (0.10 mM in **1**; open circles) while stirring at 1200 r.p.m at 25°C. (**D**) TEM micrograph of a sample in which 96% of **1** had been converted to $\mathbf{1}_3$. (**E**) HS-AFM images recorded at different times of a fiber growing on a mica surface. (**F**) Image of the growing fiber indicating the line (in green) selected to create the time-resolved intensity kymograph in (**G**). Scale bars in (**E**) and (**F**) are 50 nm. (**G**) Kymograph of the selected line section in (F) over 180 s, indicating an average growth rate of 0.5 ± 0.1 nm/s (N = 9).

In the absence of agitation, in a fully oxidized DCL prepared from **1**, macrocycle $\mathbf{1}_3$ was only a relatively minor product (Figure 1B), suggesting that shear forces promote the formation of the $\mathbf{1}_3$ fibers. This observation is in line with the fiber growth-breakage mechanism suggested previously for replicator $\mathbf{1}_6$.[36] High-speed Atomic Force Microscopy (HS-AFM) analysis[41] confirmed that $\mathbf{1}_3$ fibers continue growing from their ends after breaking the fibers using the AFM tip (Video S1, Figure S29).

The growth of $\mathbf{1}_3$ exhibits a pronounced lag phase (Figure 2A), as expected for a process of self-replication. Self-replication was confirmed through a seeding experiment, in which a small amount of $\mathbf{1}_3$ fiber was added to the solution at the start of the experiment and found to accelerate its own formation (Figure 2C; see Figure S39 for a repeat of this experiment).

We probed the relative thermodynamic stabilities of the $\mathbf{1}_3$ and $\mathbf{1}_6$ fibers by treating a mixture of the two replicators with a small amount of tris(2-carboxyethyl)phosphine (TCEP) reducing agent to promote thiolate-mediated disulfide exchange. In the absence of agitation the amount of $\mathbf{1}_3$ diminished while the amount of $\mathbf{1}_6$ grew (Figure S32), indicating that, under these conditions, the fibrous assemblies of $\mathbf{1}_6$ are thermodynamically more stable than those of $\mathbf{1}_3$.

Replication efficiencies of $\mathbf{1}_3$ and $\mathbf{1}_6$ at different oxidation levels

As we suspected, the oxidation level of the solution was found to play a key role in determining whether replicator $\mathbf{1}_3$ or $\mathbf{1}_6$ became the dominant product in a closed system. We set up a series of experiments at different oxidation levels, reflected in different thiol:disulfide ratios (expressed as % disulfide) in which equimolar amounts of pre-formed $\mathbf{1}_3$ or $\mathbf{1}_6$ replicator were supplied with excess "food" (a mixture of pre-oxidized non-fibrous macrocycles). We then determined the replicator composition after most of the "food" had been converted to replicator. Figure 3A shows an abrupt changeover in the resulting product distribution from hexamer to trimer replicator as the oxidation level increased from 95% to 98%. We attribute this changeover to a combination of two effects.

The first effect relates to the nature of the precursors from which the replicators grow, which changes with the oxidation level of the sample. We have previously shown that these precursors form non-fibrous aggregates.[41] Indeed, dynamic light scattering experiments on pre-oxidized precursor solution at different oxidation levels confirmed the presence of aggregates of 3 – 4 nm diameter (Figure S23)

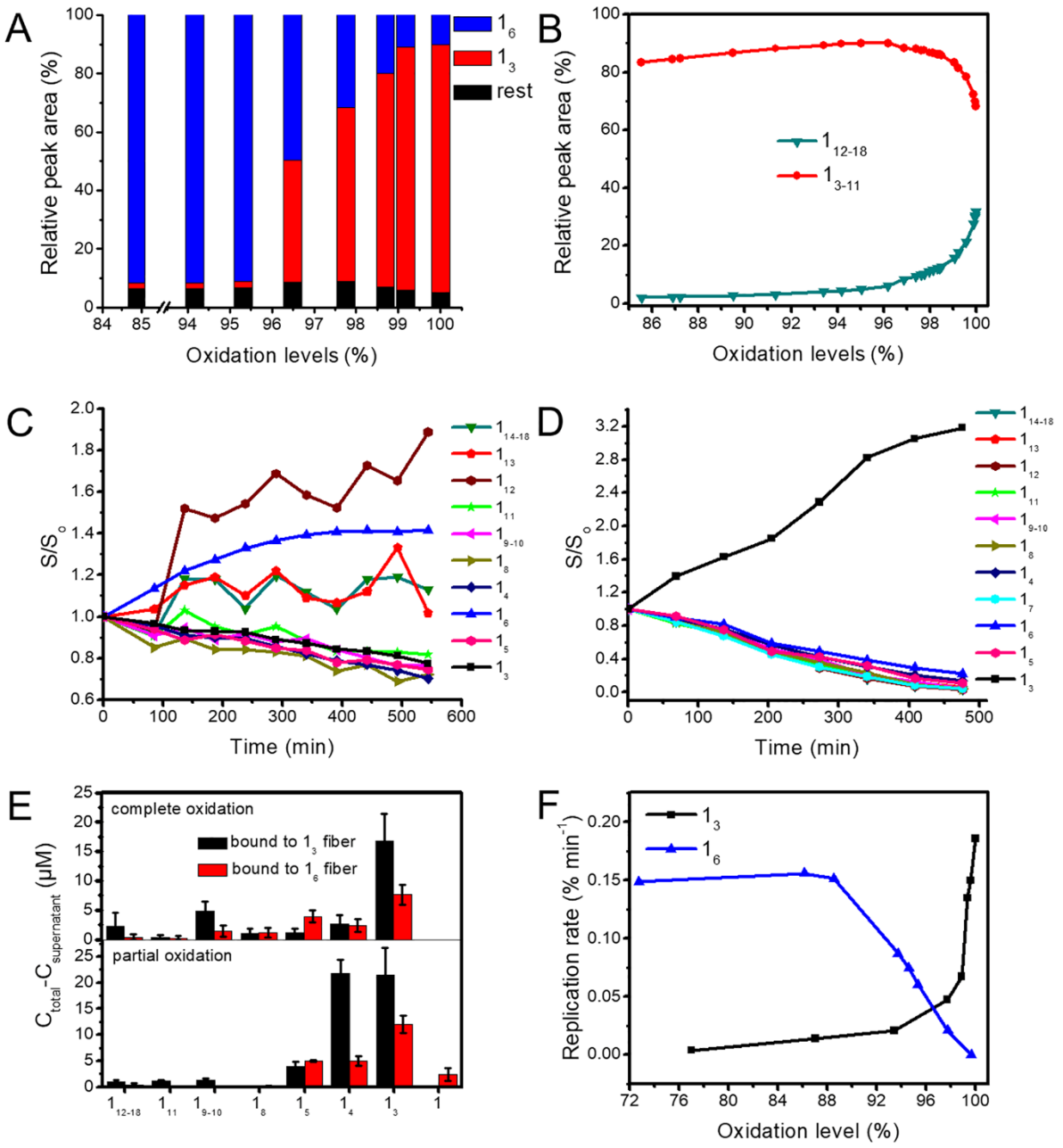

Figure 3. The oxidation level of the solution controls the outcome of replicator competition. (**A**) Final distribution of the replicators **1**$_3$ and **1**$_6$ upon supplying an equimolar mixture of both (each 25 μM in **1**) with excess preoxidized "food" (0.20 mM in **1**) at different oxidation levels (expressed as % disulfide) in borate buffer (50 mM, pH 8.2 stirred at 1200 r.p.m at 25°C; for UPLC data, see Figure S24 and Table S1). (**B**) Composition of the "food" solution (1.0 mM in **1**) at different oxidation levels. (**C**) Relative change in sample composition upon growth of replicator **1**$_6$ in a sample containing preoxidized "food" (0.20 mM in **1**) and preformed **1**$_6$ (50 μM in **1**) in borate buffer (50 mM, pH 8.2) while stirring at 1200 r.p.m. The concentration of

each species (*S*) is normalized by dividing over its concentration at $t = 0$ (S_0). The amount of monomer is 4.62% at t_0 based on the relative UPLC peak area. Note that the peak of $\mathbf{1}_7$ cannot be accurately integrated as it partially overlaps with the large $\mathbf{1}_6$ peak, but $\mathbf{1}_7$ disappeared with the growth of $\mathbf{1}_6$. (**D**) Relative change in sample composition upon growth of replicator $\mathbf{1}_3$ in a sample containing fully oxidized "food" (0.20 mM in **1**) and preformed $\mathbf{1}_3$ (50 μM in **1**) in borate buffer (50 mM, pH 8.2) while stirring at 1200 r.p.m at 25°C. (**E**) Concentration of the bound "food" on $\mathbf{1_3}$ and $\mathbf{1_6}$ fibers at different oxidation levels, for details see Figures S25 and S26. (**F**) Initial rate of self-replication of $\mathbf{1}_3$ and $\mathbf{1}_6$ at different oxidation levels. The underlying kinetic data is shown in Figures S35 and S36.

The molecular composition of the precursor solution was analyzed by UPLC. At low oxidation level it was dominated by small macrocycles whereas a collection of large macrocycles (containing from 12 to 18 monomer units) became prevalent at oxidation levels from 98 to 100 % (Figure 3B, Figure S24, Table S1). The appearance of these large macrocycles coincides with the oxidation level at which the trimer replicator becomes dominant over the hexamer (Figure 3A). These observations suggest that trimers and hexamers grow from different precursors (Figure 1). Further support for this hypothesis came from monitoring the rate at which the various precursor macrocycles disappear upon growth of the trimer or hexamer replicator. The hexamer grows from 3-11 ring precursors, without depleting the concentration of the 12-18 rings (Figure 3C). In contrast, growth of the trimer is accompanied by a reduction of nearly all precursors to a similar extent (Figure 3D).

Recent high-speed AFM studies revealed that hexamer fiber growth occurs through the formation of precursor aggregates on the sides of the fibers.[41] The nature of the material attached to the fibers was analyzed after centrifugation of a sample containing hexamer replicator fibers and precursors. The sedimented material contained, besides the hexamer, mainly 3-5 membered oligomers, also when the precursor solution contained significant amounts of 8-18mers (Figure 3E, Figure S25). Control experiments on precursor solution in the absence of fibers did not induce appreciable sedimentation (Figure S27), implying that the sedimented precursors were bound to the replicator fibers. Analogous experiments on

trimer replicator containing samples indicated that also this replicator binds precursors (Figure 3E, Figure S26). It appears to do so in a different way than the hexamer, since we were unable to detect distinct mobile replicator-bound precursor aggregates on the fiber surface by high-speed AFM as we did previously for the hexamer[41] (Figure 2E-G, video S2). We also found that the trimer replicator is able to bind the 8-18 ring precursors more efficiently than the hexamer replicator (Figure 3E). We speculate that this binding allows the trimer to grow efficiently from the large-ring precursors that become available at high oxidation level, which may account for the dominance of the trimer under these conditions.

There is potentially a second effect that accounts for trimer dominating at high oxidation level, which is related to the observation that the two competing replicators rely on different disulfide exchange mechanisms. This difference is apparent from the strikingly dissimilar dependence of the initial rate of replication of trimer and hexamer on the concentration of thiols (Figure 3F). The drop in the rate of replication of $\mathbf{1}_6$ as the oxidation level increases suggests that $\mathbf{1}_6$ replication relies on the thiol-disulfide exchange reaction, which depends critically on the presence of thiolate anion.[42]

We observed previously that $\mathbf{1}_6$ grows from aggregates bound on the fibers formed by this replicator.[41] Because of the finite size of these aggregates the number of aggregates that do not contain any thiol increases non-linearly with increasing oxidation level (see Figure S28 for a quantitative analysis) in good agreement with the non-linear dependence of $\mathbf{1}_6$ replication on oxidation level. In contrast, replication of $\mathbf{1}_3$ is likely to occur through a radical pathway (Figure S37, vide supra) and appears to be inhibited by thiols (Figure 3E). This effect may be analogous to the well-known capability for thiols to act as chain transfer agents in radical polymerization,[43] where a radical center abstracts a hydrogen from a thiol. We speculate that dithiol monomer **1** reacts similarly with any radicals that are present among the precursors on the $\mathbf{1}_3$ fibers, giving rise to a new thiol radical centered on **1**. Given that **1** does not bind efficiently to the trimer fiber (remarkably, no monomer was detected in the sediment upon centrifugation of a 80% oxidized mixture of trimer replicator and precursors;

see Figure S26c,d), it effectively transports radicals away from these fibers. The fact that monomer does not appear to bind to fibers of $\mathbf{1}_3$, while it is present on fibers of $\mathbf{1}_6$, may also explain why $\mathbf{1}_3$ fibers do not appear to grow through thiol-mediated disulfide exchange. In addition, fibers of $\mathbf{1}_3$ are more readily degraded by monomer **1** than fibers of $\mathbf{1}_6$ (Figure S38), which may further contribute to the sluggish growth of the former at low oxidation levels. Finally, we attribute the observation that $\mathbf{1}_6$ replicates predominantly through the thiolate-mediated exchange to the fact that this exchange process (requiring seconds at low millimolar concentrations of both reaction partners)[27] is normally faster than radical-mediated exchange (requiring hours at high millimolar disulfide concentrations under ambient conditions).[38] Apparently, after shutting down the rapid thiol-mediated replication pathway for $\mathbf{1}_6$, the slower radical mediated pathway for this replicator is unable to compete with radical-mediated replication of $\mathbf{1}_3$.

Replicators $\mathbf{1_3}$ and $\mathbf{1_6}$ are cross-catalytic and mutants of each other

Having established that the $\mathbf{1_3}$ and $\mathbf{1_6}$ replicators are differently affected by the oxidation state of the solution, we then investigated the extent to which they can cross-catalyze each other's formation. We first probed whether addition of fibers of $\mathbf{1_3}$ can promote the formation of replicator $\mathbf{1}_6$. Indeed, upon mixing $\mathbf{1}_3$ with **1,** replicator $\mathbf{1_6}$ was able to grow (Figure 4A) and did so more efficiently than in the absence of $\mathbf{1}_3$ (Figure 4B). Repeating these experiments gave similar results (Figure S40), albeit at a lower oxidation state replicator $\mathbf{1_3}$ was slowly depleted (Figure S33). Conversely, when replicator $\mathbf{1}_6$ was added to the solution of oxidized "food", $\mathbf{1}_3$ grew, at the expense of the other species in solution (Figure 4C) and did so more efficiently than in the absence of replicator $\mathbf{1}_6$ (Figure 4D; see Figure S41 for a repeat of this experiment).

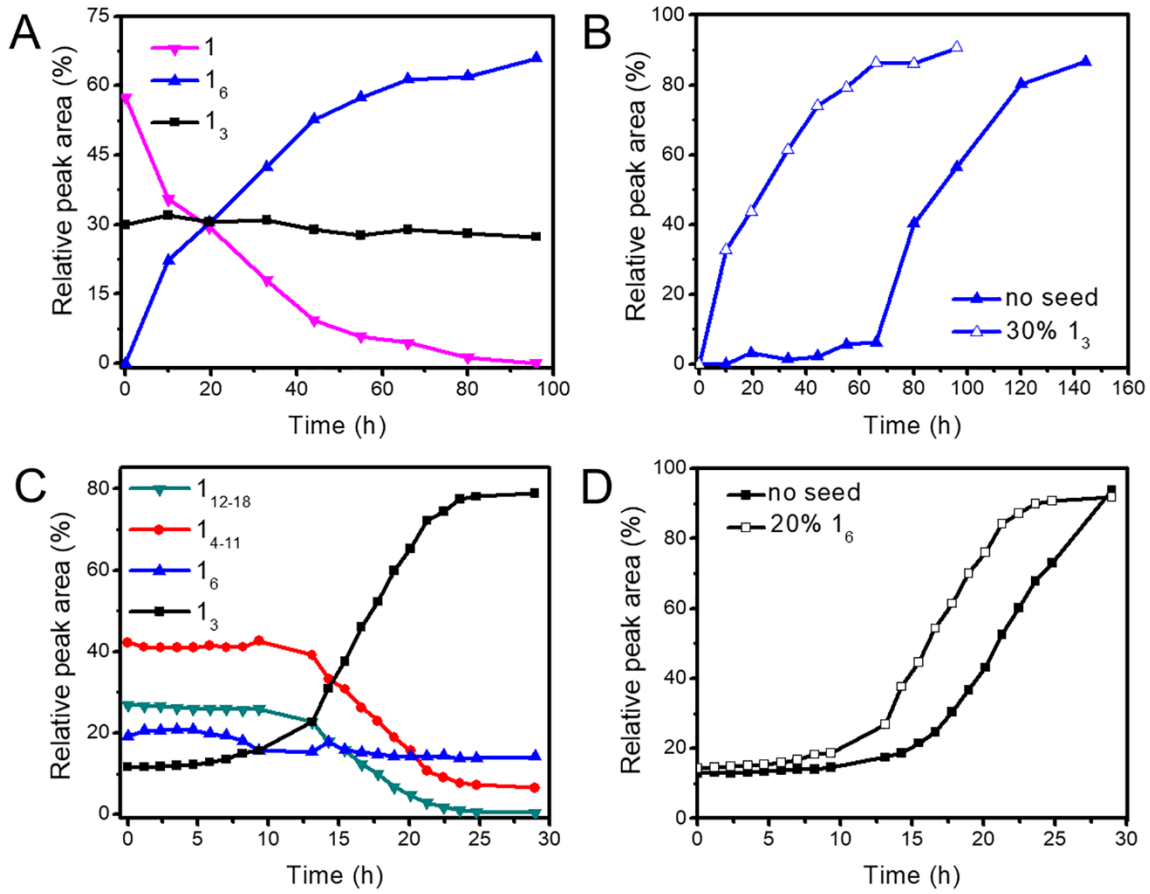

Figure 4. Cross-catalysis between replicators $\mathbf{1}_3$ and $\mathbf{1}_6$. (**A**) Growth of $\mathbf{1}_6$ upon seeding at t = 0 with preformed $\mathbf{1}_3$ (0.10 mM in **1**) in a solution containing **1** (0.20 mM) in borate buffer (50 mM, pH 8.2) under stirring at 1200 r.p.m at 25°C. (**B**) Comparison of the growth of $\mathbf{1}_6$ in the absence (solid triangles) and presence (open triangles) of seed. Conditions and seeding as described for (A). (**C**) Growth of $\mathbf{1}_3$ upon seeding at t = 0 with preformed $\mathbf{1}_6$ (0.05 mM in **1**) in a solution containing fully oxidized "food" (0.20 mM in **1**) in borate buffer (50 mM, pH 8.2) under stirring at 1200 r.p.m at 25°C. (**D**) Comparison of the growth of $\mathbf{1}_3$ in the absence (solid squares) and presence (open squares) of seed. Conditions and seeding as described for (C).

Thus, the two replicators can promote each other's formation. Such behavior can be interpreted as a mutation,[13] where we define mutation as an alteration in the heritable information contained in a replicating entity that is more or less permanent and that can be

transmitted to the entities' descendants. In the present system the heritable information is the size of the ring that self-replicates (as shown by seeding experiments). This information is altered (involving promotion of the formation of a new ring size by an existing ring size). This new ring size is transmitted to the descendants (as also evident from our data) more or less permanently, until environmental conditions change (see below).

Replicators $\mathbf{1}_3$ and $\mathbf{1}_6$ can change their environment by photoredox catalysis

Having identified a system of replicator mutants $\mathbf{1}_3$ and $\mathbf{1}_6$ that compete for a common building block but have different replication efficiencies at different oxidation levels, we investigated their ability to recruit and activate a photoredox cofactor and thereby alter the redox level of their environment. We chose pheophorbide A (**2**, Figure 5A), a well-known photosensitizer,[44] as the photocatalytic cofactor. This cofactor was chosen over the ones we identified previously[32] as it is more efficient at generating singlet oxygen,[45] which promotes the oxidation of thiols into disulfides. The Soret absorption band of **2** red-shifted from 395 nm in buffer solution to 406 nm in the presence of the either replicator (Figure S19), suggesting that the dye binds to the replicator fibers. Separate experiments probing the fluorescence of 8-anilino-1-naphthalene-sulfonic acid (ANS), known to bind through hydrophobic interactions,[46] indicate the presence hydrophobic domains on the fibers surface (Figure S20). We speculate that **2** binds to the replicator fibers through a combination of hydrophobic interactions and electrostatic interactions between the carboxylate group of **2** and the protonated lysines on the fibers. The fluorescence intensity of **2** was increased 2.0 and 3.3 times upon binding to replicators $\mathbf{1_6}$ and $\mathbf{1_3}$, respectively (Figure 5A). The enhancement of fluorescence can be attributed to the alleviation of aggregation-induced self-quenching allowing for a longer-lived excited state. We measured the efficiency of photocatalytic singlet oxygen production by the cofactor-replicator combinations using 9,10-anthracenediyl-bis(methylene)dimalonic acid as a probe.[47] The production rate of singlet oxygen was enhanced by 4.1 and 4.4 times upon binding to replicators $\mathbf{1_6}$ and $\mathbf{1_3}$, respectively (Figure 5B),

indicating that the efficiency with which excited state energy was transferred to the triplet state, and subsequently used for excitation of triplet oxygen, was enhanced by binding to the replicator fibers. The rate of oxidation of **1** was enhanced 2.1-fold or 2.3-fold upon binding of **2** to replicator $\mathbf{1_6}$ or $\mathbf{1_3}$, respectively (Figure 5C), indicating partial usage of singlet oxygen for oxidizing thiols into disulfide. A series of control experiments showed that irradiation, replicator and cofactor are all playing a role in achieving the observed photoredox catalysis (Figure 5C). AFM images showed that **2** did not induce noticeable changes in the fibrous assemblies of the replicators (Figure S22).

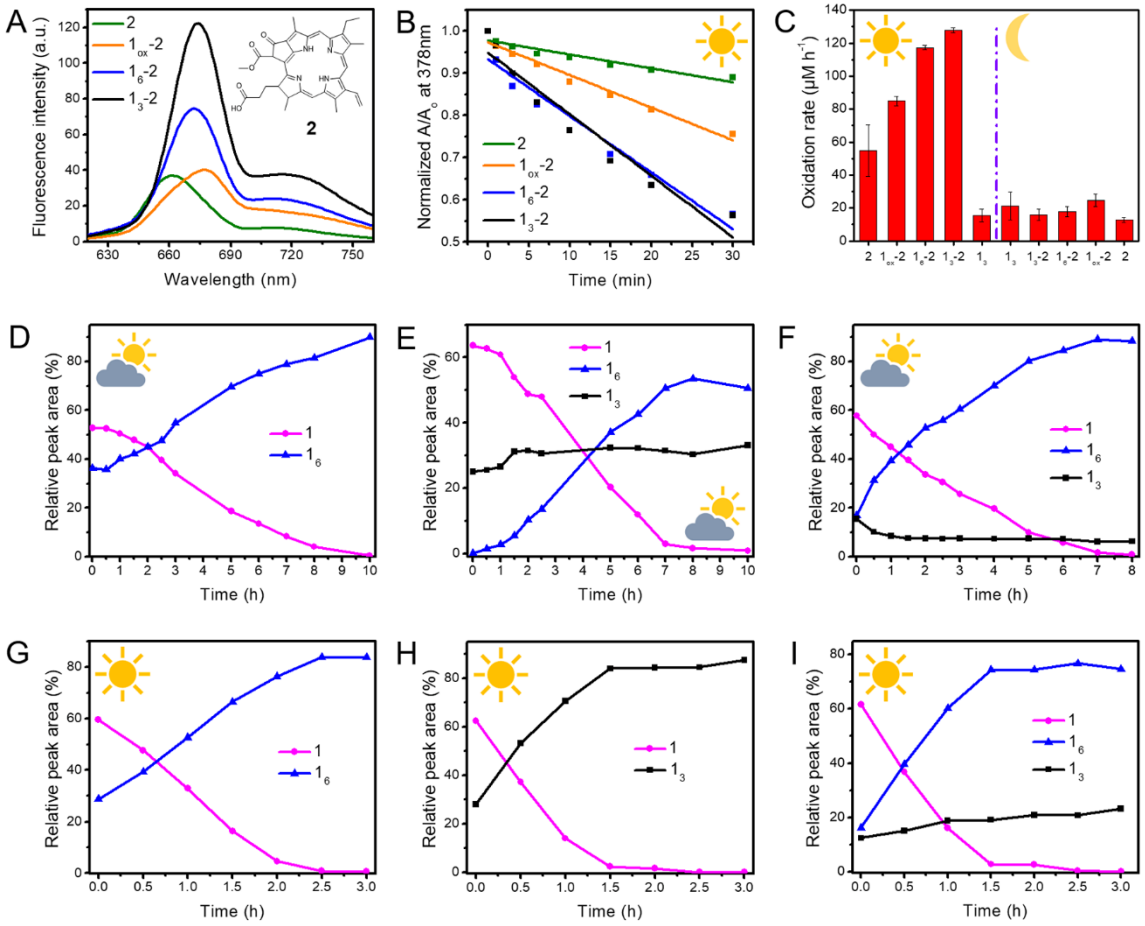

Figure 5. Replicator-mediated activation of cofactor **2** and photocatalytic self-replication. (**A**) Fluorescence spectra of **2** (4.0 μM) in the presence of $\mathbf{1}_6$ (0.20 mM in **1**) or $\mathbf{1_3}$ (0.20 mM in **1**) in borate buffer (50 mM, pH 8.2). (**B**) Relative changes of 9,10-anthracenediyl-

bis(methylene)dimalonic acid (ABDA) concentration in samples containing **2** in the absence or presence of "food", replicator $\mathbf{1}_6$, or replicator $\mathbf{1}_3$ in borate buffer upon photoirradiation ("strong light" regime). The absorbance of ABDA (A) is normalized by dividing over its absorbance at t = 0 (A_0). (**C**) Initial rates of oxidation of **1** in samples containing **2** in the absence or presence of "food", replicator $\mathbf{1}_6$, or replicator $\mathbf{1}_3$ in borate buffer upon photoirradiation ("strong light" regime). Data is also shown for control experiments performed in absence of light, **2** or fibers. (**D**) Exposing a solution containing $\mathbf{1}_6$ (0.20 mM in **1**), **1** (0.20 mM), and **2** (4.0 μM) to weak light resulted in efficient replication of $\mathbf{1}_6$. (**E**) Exposing a solution containing $\mathbf{1}_3$ (0.20 mM in **1**), **1** (0.20 mM), and **2** (4.0 μM) to weak light led to the emergence of $\mathbf{1}_6$. (**F**) Competition between replicators $\mathbf{1}_6$ (0.10 mM in **1**) and $\mathbf{1}_3$ (0.10 mM in **1**) for building block **1** (0.20 mM) in the presence of **2** (4.0 μM) in weak light. (**G**) Repeat of the experiment in D under strong light. (**H**) Repeat of the experiment in E under strong light. (**I**) Repeat of the experiment in F under strong light. All samples were prepared in borate buffer (50 mM, pH 8.2) and stirred at 1200 r.p.m at room temperature.

Photocatalysis was also found to promote the replication of $\mathbf{1}_6$ which is now completed in 10 hours (Figure 5D; see Figure S42A for a repeat), where this took approximately 80 hours in the absence of photocatalysis (Figure 4B). These results were obtained while irradiating with light of modest intensity ("weak light" regime; see experimental section for a more quantitative description). Increasing light intensity ("strong light" regime) further enhanced the rate of oxidation and subsequent replication (Figure 5G; note the different x-axis scale; see Figure S42B for a repeat). We performed similar experiments starting from replicator $\mathbf{1}_3$. Upon mixing it with building block **1** and cofactor **2** and exposure to weak light, this replicator barely grew. Instead competing replicator $\mathbf{1}_6$ emerged and became the dominant product (Figure 5E; see Figure S43A for a repeat). These results are in agreement with replicator $\mathbf{1}_3$ promoting the formation of $\mathbf{1}_6$ as observed previously (Figure 4A and B). In the "strong light" regime a very different outcome was observed: replicator $\mathbf{1}_3$ grew efficiently and no $\mathbf{1}_6$ was observed (Figure 5H; see Figure S43B for a repeat). The more intense irradiation results in a higher oxidation level being attained faster, which benefits replicator $\mathbf{1}_3$ as we have shown above. The effect of the different irradiation conditions on the replication rates of $\mathbf{1}_3$ and $\mathbf{1}_6$ is summarized in Figure S31.

We also placed the two replicators in competition. Irradiating a mixture of $\mathbf{1}_6$, $\mathbf{1}_3$, **1**, and **2** led to efficient growth of replicator $\mathbf{1}_6$ in the “weak light” and “strong light” regimes (see Figure 5F and I, respectively; see Figure S44 for repeats). Replicator $\mathbf{1}_3$ diminished under weak light and showed modest growth under strong light. Note that at the start of these experiments the oxidation level is relatively low (50%) but as the experiment progresses the oxidation level increases. As expected the growth of replicator $\mathbf{1}_6$ stalls at high oxidation level, while the growth of $\mathbf{1}_3$ is less affected (Figure 5I). Under the reaction conditions fibers $\mathbf{1}_3$ and $\mathbf{1}_6$ were comparable in length, suggesting that they have similar fragmentation tendencies (Figure S21). Therefore, the outcome of the competition is primarily determined by differences in fiber growth rates, which are a function of the environment.

Replicators adapt to the changes in the environment that they induce

All experiments above were conducted in closed systems, yielding kinetically determined product distributions. In order to probe evolutionary dynamics we subjected the competing replicators to a replication-destruction regime, continuously supplying them with building block **1**, while continuously removing part of the solution. This was implemented using a continuously stirred tank reactor (CSTR) setup shown in Figure 6A. Also cofactor **2** was continuously supplied to ensure it is present at a constant concentration. At the start of the experiments we placed a mixture of replicators $\mathbf{1}_3$ and $\mathbf{1}_6$ into the CSTR. Upon starting the in- and outflow (turnover time 16.7 h) and exposure to weak light, the concentration of both replicators initially diminished (stage 1**,** Figure 6B). At this stage the concentration of cofactor **2** is still building up and photooxidation and replication cannot keep up with the outflow of the replicators. However, as more **2** accumulates, the photooxidation rate increases and replicator $\mathbf{1}_6$ grew rapidly to become the dominant product after 35 hours (stage 2, Figure 6B). The population of replicator $\mathbf{1}_6$ then reached a steady state (stage 3, Figure 6B). When at t = 105 h the light was switched off, photocatalysis was no longer possible and the replicators rapidly declined. These results are consistent with the behavior of the replicators in a closed

vial (Figure 5F). Thus, in the replication-destruction regime under weak light replicator $\mathbf{1}_6$ has the highest dynamic kinetic stability.[25,26] Under these conditions the replicator with highest dynamic kinetic stability happens to also be the replicator that is thermodynamically most stable.

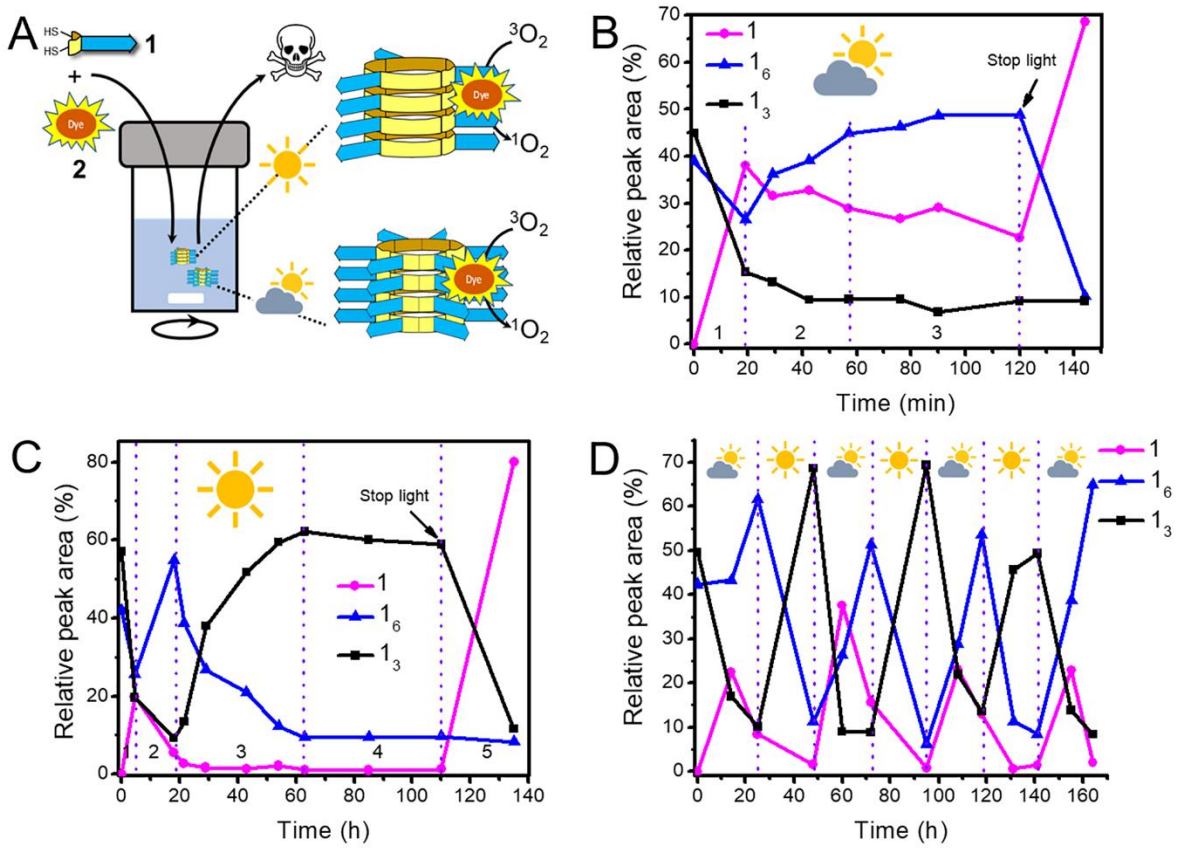

Figure 6. Ecological-evolutionary dynamics. (**A**) Schematic of the CSTR setup. The reactor is charged with 500 µL of an equimolar solution of replicators $\mathbf{1_6}$ and $\mathbf{1_3}$ (1.0 mM in **1** in total) and solutions of building block **1** (1.0 mM) and cofactor **2** (10 µM) are continuously supplied (15 µL h^{-1} each) accompanied by continuous outflow (30 µL h^{-1}) while irradiating with (**B**) weak light, (**C**) strong light, and (**D**) alternating between weak and strong light. Dotted lines are used to differentiate reaction stages and/or mark the change of light intensity in (**D**). All solutions contain borate buffer (50 mM, pH 8.2) and were stirred at 1200 r.p.m at room temperature. Data obtained upon repeating these experiments are shown in Figures S45-47.

When the same flow experiment was repeated under strong light, the samples initially behaved similar to what was observed under weak light, albeit on a somewhat shorter timescale, due to faster photo-oxidation. Initial decline of the two replicators (stage 1, Figure 6C) was, again, followed by an increase in the amount of replicator $\mathbf{1}_6$ (stage 2; Figure 6C). However, the dominance of $\mathbf{1}_6$ was now only transient, as replicator $\mathbf{1}_3$ took over after 20 h. Photooxidation, mediated mostly by replicator $\mathbf{1}_6$, caused the oxidation level to increase, changing the environment into one that selectively benefits the competing replicator $\mathbf{1}_3$, causing this replicator to partially displace $\mathbf{1}_6$ (stage 3 in Figure 6C). This behavior represents an example of ecological-evolutionary dynamics. A steady state rich in $\mathbf{1}_3$ is then reached (stage 4 in Figure 6C). As expected, halting irradiation causes replicator demise (stage 5). The behaviors observed in Figure 6B and 6C were qualitative reproducible (Figure S45 and S46).

Finally, we probed the extent to which this dynamic system of competing replicators can adapt to changing environmental conditions by alternating between strong and weak light. Starting under weak light, replicator $\mathbf{1}_6$ became dominant, as expected (Figure 6D). Changing to strong light resulted in a more oxidized environment, thereby favoring replicator $\mathbf{1}_3$ in a process similar to natural selection:[46] there is variation among replicators ($\mathbf{1}_3$ and $\mathbf{1}_6$), which is heritable (Fig.3), and reproduction and decay depend on the environment. The adaptation to changing environmental conditions occurred consistently upon several alternations between weak and strong light (Figure 6D and Figure S47 for independent repeats of this experiment).

Conclusions

We developed a minimal system of two mutant self-replicators $\mathbf{1}_3$ and $\mathbf{1}_6$ that compete for a common building block. These replicators can recruit a cofactor and activate it with

comparable efficiencies, enabling them to modulate the oxidation level of their environment through photoredox catalysis. As the replication efficiency of the two replicators is different at different oxidation levels, ecological-evolutionary dynamics arise that are conceptually similar to that encountered in living systems, but did not yet have an equivalent outside biology. Specifically, irradiating a mixture of the two replicators at relatively high light intensity first allowed $\mathbf{1}_6$ to dominate. However, the photoredox activity of this replicator caused an increase of the oxidation level of the environment that led to its own demise, making room for the dominance of the competing replicator $\mathbf{1}_3$. Decreasing light intensity reduced photoredox catalysis and led to a lower oxidation level and a resurgence of $\mathbf{1}_6$ at the expense of $\mathbf{1}_3$. Thus, different replicator populations are selected based on their dynamic kinetic stability, where photoirradiation enables overriding thermodynamic preferences.

The adaptation of the replicator system to a changing environment involves the processes of mutation (the two replicators are cross-catalytic) and selection. Adaptation through mutation and selection represents the cornerstone of Darwinian evolution and is exhibited here, outside the realm of biology, in a minimal replicator systems. Such systems represent important stepping stones to the future use of Darwinian methods for evolving synthetic chemical systems towards desired properties and to the de-novo synthesis of life.

References

(1) Miikkulainen, R.; Forrest, S. A biological perspective on evolutionary computation *Nat. Mach. Intell.* **2021**, *3*, 9-15.
(2) Zeymer, C.; Hilvert, D. Directed evolution of protein catalysts *Annu. Rev. Biochem.* **2018**, *87*, 131-157.
(3) Arnold, F. H. Directed evolution: Bringing new chemistry to life *Angew. Chem. Int. Ed.* **2018**, *57*, 4143-4148.
(4) Adamski, P.; Eleveld, M.; Sood, A.; Kun, A.; Szilagyi, A.; Czaran, T.; Szathmary, E.; Otto, S. From self-replication to replicator systems en route to de novo life *Nat. Rev. Chem.* **2020**, *4*, 386-403.
(5) Jakiela, S.; Kaminski, T. S.; Cybulski, O.; Weibel, D. B.; Garstecki, P. Bacterial growth and adaptation in microdroplet chemostats *Angew. Chem. Int. Ed.* **2013**, *52*, 8908-8911.
(6) Behe, M. J. Experimental evolution, loss-of-function mutations, and "the first rule of adaptive evolution" *Q. Rev. Biol.* **2010**, *85*, 419-445.
(7) Mizuuchi, R.; Ichihashi, N.; Yomo, T. Adaptation and diversification of an rna replication system under initiation- or termination-impaired translational conditions *ChemBioChem* **2016**, *17*, 1229-1232.
(8) Govaert, L.; Fronhofer, E. A.; Lion, S.; Eizaguirre, C.; Bonte, D.; Egas, M.; Hendry, A. P.; Martins, A. D.; Melian, C. J.; Raeymaekers, J. A. M.; Ratikainen, II; Saether, B. E.; Schweitzer, J. A.; Matthews, B. Eco-evolutionary feedbacks-theoretical models and perspectives *Funct. Ecol.* **2019**, *33*, 13-30.
(9) Schoener, T. W. The newest synthesis: Understanding the interplay of evolutionary and ecological dynamics *Science* **2011**, *331*, 426-429.
(10) Kosikova, T.; Philp, D. Exploring the emergence of complexity using synthetic replicators *Chem. Soc. Rev.* **2017**, *46*, 7274-7305.
(11) Clixby, G.; Twyman, L. Self-replicating systems *Org. Biomol. Chem.* **2016**, *14*, 4170-4184.
(12) Le Vay, K.; Weise, L. I.; Libicher, K.; Mascarenhas, J.; Mutschler, H. Templated self-replication in biomimetic systems *Adv. Biosyst.* **2019**, *3*, 1800313.
(13) Hong, J. I.; Feng, Q.; Rotello, V.; Rebek, J. Competition, cooperation, and mutation - improving a synthetic replicator by light irradiation *Science* **1992**, *255*, 848-850.
(14) Yao, S.; Ghosh, I.; Zutshi, R.; Chmielewski, J. A pH-modulated, self-replicating peptide *J. Am. Chem. Soc.* **1997**, *119*, 10559-10560.
(15) Yao, S.; Ghosh, I.; Zutshi, R.; Chmielewski, J. A self-replicating peptide under ionic control *Angew. Chem. Int. Ed.* **1998**, *37*, 478-481.
(16) Leonetti, G.; Otto, S. Solvent composition dictates emergence in dynamic molecular networks containing competing replicators *J. Am. Chem. Soc.* **2015**, *137*, 2067-2072.
(17) Dadon, Z.; Samiappan, M.; Wagner, N.; Ashkenasy, G. Chemical and light triggering of peptide networks under partial thermodynamic control *Chem. Commun.* **2012**, *48*, 1419-1421.
(18) Dadon, Z.; Samiappan, M.; Safranchik, E. Y.; Ashkenasy, G. Light-induced peptide replication controls logic operations in small networks *Chem.-Eur. J.* **2010**, *16*, 12096-12099.
(19) Riess, B.; Grotsch, R. K.; Boekhoven, J. The design of dissipative molecular assemblies driven by chemical reaction cycles *Chem* **2020**, *6*, 552-578.
(20) Ragazzon, G.; Prins, L. J. Energy consumption in chemical fuel-driven self-assembly *Nat. Nanotech.* **2018**, *13*, 882-889.
(21) Merindol, R.; Walther, A. Materials learning from life: Concepts for active, adaptive and autonomous molecular systems *Chem. Soc. Rev.* **2017**, *46*, 5588-5619.
(22) Sorrenti, A.; Leira-Iglesias, J.; Markvoort, A. J.; de Greef, T. F. A.; Hermans, T. M. Non-equilibrium supramolecular polymerization *Chem. Soc. Rev.* **2017**, *46*, 5476-5490.
(23) Engwerda, A. H. J.; Southworth, J.; Lebedeva, M. A.; Scanes, R. J. H.; Kukura, P.; Fletcher, S. P. Coupled metabolic cycles allow out-of-equilibrium autopoietic vesicle replication *Angew. Chem. Int. Ed.* **2020**, *59*, 20361-20366.

(24) Morrow, S. M.; Colomer, I.; Fletcher, S. P. A chemically fuelled self-replicator *Nat. Commun.* **2019**, *10*, 1011.
(25) Pross, A. Seeking to uncover biology's chemical roots *Emerg. Top. Life Sci.* **2019**, *3*, 435-443.
(26) Pross, A. *What is life? How chemistry becomes biology*; Oxford University Press: Oxford, 2012.
(27) Yang, S.; Schaeffer, G.; Mattia, E.; Markovitch, O.; Liu, K.; Hussain, A. S.; Ottelé, J.; Sood, A.; Otto, S. Chemical fueling enables molecular complexification of self-replicators *Angew. Chem. Int. Ed.* **2021**, *60*, 11344-11349.
(28) Bandela, A. K.; Wagner, N.; Sadihov, H.; Morales-Reina, S.; Chotera-Ouda, A.; Basu, K.; Cohen-Luria, R.; de la Escosura, A.; Ashkenasy, G. Primitive selection of the fittest emerging through functional synergy in nucleopeptide networks *Proc. Natl. Acad. Sci. U. S. A.* **2021**, *118*, e2015285118.
(29) Wagner, N.; Hochberg, D.; Peacock-Lopez, E.; Maity, I.; Ashkenasy, G. Open prebiotic environments drive emergent phenomena and complex behavior *Life* **2019**, *9*, 45.
(30) Kamioka, S.; Ajami, D.; Rebek, J. Autocatalysis and organocatalysis with synthetic structures *Proc. Natl. Acad. Sci. USA* **2010**, *107*, 541-544.
(31) Arsene, S.; Ameta, S.; Lehman, N.; Griffiths, A. D.; Nghe, P. Coupled catabolism and anabolism in autocatalytic rna sets *Nucleic Acids Res.* **2018**, *46*, 9660-9666.
(32) Santiago, G. M.; Liu, K.; Browne, W. R.; Otto, S. Emergence of light-driven protometabolism on recruitment of a photocatalytic cofactor by a self-replicator *Nat. Chem.* **2020**, *12*, 603-607.
(33) Ottele, J.; Hussain, A. S.; Mayer, C.; Otto, S. Chance emergence of catalytic activity and promiscuity in a self-replicator *Nat. Catal.* **2020**, *3*, 547-553.
(34) Black, S. P.; Sanders, J. K. M.; Stefankiewicz, A. R. Disulfide exchange: Exposing supramolecular reactivity through dynamic covalent chemistry *Chem. Soc. Rev.* **2014**, *43*, 1861-1872.
(35) Malakoutikhah, M.; Peyralans, J. J. P.; Colomb-Delsuc, M.; Fanlo-Virgos, H.; Stuart, M. C. A.; Otto, S. Uncovering the selection criteria for the emergence of multi-building-block replicators from dynamic combinatorial libraries *J. Am. Chem. Soc.* **2013**, *135*, 18406-18417.
(36) Colomb-Delsuc, M.; Mattia, E.; Sadownik, J. W.; Otto, S. Exponential self-replication enabled through a fibre elongation/breakage mechanism *Nat. Commun.* **2015**, *6*, 7427.
(37) Rekondo, A.; Martin, R.; de Luzuriaga, A. R.; Cabanero, G.; Grande, H. J.; Odriozola, I. Catalyst-free room-temperature self-healing elastomers based on aromatic disulfide metathesis *Mater. Horizons* **2014**, *1*, 237-240.
(38) Nevejans, S.; Ballard, N.; Miranda, J. I.; Reck, B.; Asua, J. M. The underlying mechanisms for self-healing of poly(disulfide)s *Phys. Chem. Chem. Phys.* **2016**, *18*, 27577-27583.
(39) Sreerama, N.; Woody, R. W. Computation and analysis of protein circular dichroism spectra *Methods Enzymol.* **2004**, *383*, 318-351.
(40) LeVine III, H. Thioflavine-T interaction with synthetic alzheimers-disease beta-amyloid peptides - detection of amyloid aggregation in solution *Protein Sci.* **1993**, *2*, 404-410.
(41) Maity, S.; Ottele, J.; Santiago, G. M.; Frederix, P.; Kroon, P.; Markovitch, O.; Stuart, M. C. A.; Marrink, S. J.; Otto, S.; Roos, W. H. Caught in the act: Mechanistic insight into supramolecular polymerization-driven self-replication from real-time visualization *J. Am. Chem. Soc.* **2020**, *142*, 13709-13717.
(42) Otto, S.; Furlan, R. L.; Sanders, J. K. Dynamic combinatorial libraries of macrocyclic disulfides in water. *J. Am. Chem. Soc.* **2000**, *122*, 12063-12064.
(43) Henrıquez, C.; Bueno, C.; Lissi, E.; Encinas, M. Thiols as chain transfer agents in free radical polymerization in aqueous solution. *Polymer* **2003**, 44, 5559-5561.
(44) Roder, B.; Hanke, T.; Oelckers, S.; Hackbarth, S.; Symietz, C. Photophysical properties of pheophorbide a in solution and in model membrane systems *J. Porphyrins Phthalocyanines* **2000**, *4*, 37-44.
(45) Ogilby, P. R. Singlet oxygen: There is indeed something new under the sun *Chem. Soc. Rev.* **2010**, *39*, 3181-3209.

(46) Semisotnov, G. V.; Rodionova, N. A.; Razgulyaev, O. I.; Uversky, V. N.; Gripas, A. F.; Gilmanshin, R. I. Study of the molten globule intermediate state in protein folding by a hydrophobic fluorescent-probe *Biopolymers* **1991**, *31*, 119-128.
(47) Entradas, T.; Waldron, S.; Volk, M. The detection sensitivity of commonly used singlet oxygen probes in aqueous environments *J. Photochem. Photobiol. B-Biol.* **2020**, *204*, 11.

Acknowledgements

K.L. thanks O. Markovitch (University of Groningen) for providing guidance on the usage of UPLC stirring device. This work was supported by the Simons Foundation (553330), Marie Curie Individual Fellowships (PSR 786350), the oLife Cofund program (847675), the ERC (AdG 741774), the China Scholarship Council, and the Dutch Ministry of Education, Culture and Science (Gravitation program 024.001.035).

Author contributions: K.L. and S.O. conceived the concept. K.L. designed, performed experiments and analyzed the data. A.W.P.B. assisted in the data analysis and contributed to the scientific discussion. C.E. performed the experiments related to HS-AFM. C.E. and W.H.R. analyzed the data related to HS-AFM. A.K. performed the experiments related to TEM. J.W. performed the experiments related to UPLC-MS. K.L. A.W.P.B. and S.O. wrote the manuscript.

Competing interests: There are no competing interests.

Data and materials availability: Most data are available in the manuscript or the supplementary materials. Raw data is available from the authors on reasonable request.